

Chemokines in proliferative diabetic retinopathy and proliferative vitreoretinopathy

Ahmed M. Abu El-Asrar¹, Sofie Struyf², Dustan Kangave³, Karel Geboes⁴, Jo Van Damme²

¹ Department of Ophthalmology, College of Medicine, King Saud University, Department of Ophthalmology, King Abdulaziz University Hospital, Airport Road, P.O. Box 245, Riyadh 11411, Saudi Arabia
Tel.: 966 1 477 5723; fax: 966 1 477 5724/477 5741

² Rega Institute for Medical Research, Laboratory of Molecular Immunology, University of Leuven, Belgium

³ Research Center, College of Medicine, King Saud University, Riyadh, Saudi Arabia

⁴ Laboratory of Histochemistry and Cytochemistry, University of Leuven, Leuven, Belgium

Correspondence : A.M. Abu El-Asrar
<abuasar@KSU.edu.sa>

Accepted for publication June 18, 2006

ABSTRACT. Purpose. To determine levels of the chemokines CCL1/I-309, CCL2/MCP-1, CCL3/MIP-1 α , CCL4/MIP-1 β , CCL7/MCP-3, CCL8/MCP-2, CXCL5/ENA-78, CXCL6/GCP-2, CXCL10/IP-10, and CXCL11/I-TAC in the vitreous humor and serum, from patients with proliferative diabetic retinopathy (PDR), proliferative vitreoretinopathy (PVR), and rhegmatogenous retinal detachment with no PVR (RD), and to investigate the expression of MCP-1, CXCL12/SDF-1, and the chemokine receptor CXCR3 in epiretinal membranes. **Methods.** Paired vitreous humor and serum samples were obtained from patients undergoing vitrectomy for the treatment of RD (57 specimens), PVR (32 specimens), and PDR (88 specimens). The levels of chemokines were measured by enzyme-linked immunosorbent assays. Eighteen PDR and 5 PVR membranes were studied by immunohistochemical techniques. **Results.** Of all the chemokines studied, only MCP-1 and IP-10 were detected in vitreous humor samples. MCP-1 levels in vitreous humor samples were significantly higher than in serum samples ($p < 0.001$). MCP-1 levels were significantly higher in vitreous humor samples from patients with PVR and PDR compared with RD ($p = 0.0002$). MCP-1 levels in vitreous humor samples from patients with active PDR were significantly higher than in inactive PDR cases ($p = 0.0224$). IP-10 levels in vitreous humor samples were significantly higher than in serum samples ($p = 0.0035$). IP-10 levels were significantly higher in vitreous humor samples from patients with PVR and PDR compared with RD ($p = 0.0083$). The incidence of IP-10 detection in vitreous humor samples was significantly higher in active PDR cases compared with inactive cases ($p = 0.0214$). There was a significant association between the incidence of IP-10 detection and increased levels of MCP-1 in vitreous humor samples from all patients, and patients with RD and PDR ($p < 0.001$ for all comparisons). MCP-1, and SDF-1 were localized in myofibroblasts in PVR and PDR membranes and in vascular endothelial cells in PDR membranes. CXCR3 was expressed by vascular endothelial cells in PDR membranes. **Conclusion.** MCP-1, IP-10 and SDF-1 may participate in pathogenesis of PVR and PDR. Myofibroblasts and vascular endothelial cells are the major cell types expressing MCP-1, SDF-1, and CXCR3 in epiretinal membranes.

Keywords: eye, retina, diabetic retinopathy, vitreous humor, proliferative vitreoretinopathy, chemokines

Proliferative diabetic retinopathy (PDR) is a serious complication of diabetes mellitus and is characterized by neovascularization on the retina and the development of fibrovascular membranes at the vitreoretinal interface. Formation of fibrovascular tissue often leads to substantial morbidity and blindness due to vitreous humor hemorrhage and/or traction retinal detachment. Proliferative vitreoretinopathy (PVR), a well recognized complication of rhegmatogenous retinal detachment, is characterized by the development of fibrocellular membranes on either side of the retina. The formation and gradual contraction of these membranes causes a marked distortion of the retinal architecture and results in complex retinal detachments that are difficult to repair. The pathogenesis of epiretinal membranes is still not well understood, but inflammatory and

immunological processes are known to be implicated. Several studies of epiretinal membranes showed the presence of activated T lymphocytes, B lymphocytes, and macrophages [1-3]. The specific mediators that orchestrate the recruitment of leukocytes leading to proliferative vitreoretinal disorders have not been fully elucidated, although several studies demonstrated elevated levels of several chemokines in vitreous humour removed from patients with proliferative vitreoretinal disorders [4-8]. In addition, it has been demonstrated that angiogenic growth factors, such as vascular endothelial growth factor (VEGF) play an important role in mediating ischemia-induced retinal neovascularization in PDR [9]. Recently, Watanabe *et al.* [10] demonstrated that erythropoietin is a potent ischemia-induced angiogenic factor that acts independently of VEGF during retinal angiogenesis in PDR.

Chemokines are multifunctional mediators that can direct the recruitment of leukocytes to sites of inflammation, promote inflammation, enhance immune responses, and promote stem cell survival, development, and homeostasis [11]. Recently, it was demonstrated that chemokines play a pivotal role in mediating angiogenesis and fibrosis [12–14]. They are divided into four subgroups, CXC, CC, C, and CX3C according to the arrangement of the conserved cysteine residue. In general, CC chemokines are potent chemoattractants and activators for monocytes, T lymphocytes, eosinophils, and basophils. This subfamily includes CCL1/I-309, monocyte chemoattractant protein-1 (CCL2/MCP-1), macrophage inflammatory protein-1 α (CCL3/MIP-1 α), macrophage inflammatory protein-1 β (CCL4/MIP-1 β), monocyte chemoattractant protein-3 (CCL7/MCP-3), and monocyte chemoattractant protein-2 (CCL8/MCP-2). The CXC chemokines are divided into two subgroups depending on the presence or absence of the sequence glutamic acid-leucine-arginine (ELR) that immediately precedes the first cysteine amino acid in the primary structure of these cytokines. The ELR-containing CXC chemokines, such as epithelial cell-derived neutrophil attractant-78 (CXCL5/ENA-78), and granulocyte chemotactic protein-2 (CXCL6/GCP-2) chemoattract neutrophils and are angiogenic. Most non-ELR CXC chemokines such as interferon- γ -inducible protein of 10 kDa (CXCL10/IP-10) and interferon-inducible T-cell α chemoattractant (CXCL11/I-TAC) potently chemoattract activated T lymphocytes and are angiostatic [15]. The sole reported exception of the non-ELR CXC chemokines is stromal cell-derived factor-1 (CXCL12/SDF-1), which, despite lacking an ELR motif, is angiogenic [16–18]. The effects of these chemokines depend on the presence of chemokine receptors on the target cells [11, 12, 15]. Because of the involvement of these chemokines in the recruitment of leukocytes [11], and their role in regulating angiogenesis and fibrosis [12–14], we hypothesized that their excessive production may play a role in the pathogenesis of proliferative vitreoretinal disorders.

To address mechanisms involved in the pathogenesis of proliferative vitreoretinal disorders, and to identify molecular targets for therapeutic intervention, we measured the levels of the chemokines I-309, MCP-1, MIP-1 α , MIP-1 β , MCP-3, MCP-2, ENA-78, GCP-2, IP-10, and I-TAC in the vitreous humor and serum from a series of patients with PDR, PVR, and rhegmatogenous retinal detachment with no PVR (RD). In addition, we investigated the expression of the chemokines MCP-1, and SDF-1, and the chemokine receptor CXCR3 in the epiretinal membranes from patients with PDR, and PVR. The level of vascularization and proliferative activity in epiretinal membranes were determined by immunodetection of the panendothelial marker CD34, and the myofibroblast marker α -smooth muscle actin (α -SMA).

MATERIALS AND METHODS

Vitreous humor samples and epiretinal membrane specimens

Vitreous humor and paired serum samples were obtained from 177 consecutive patients (177 eyes) undergoing vit-

rectomy for the treatment of RD (57 specimens), PVR (32 specimens), and PDR (88 specimens). All PVR cases were grade C3 or worse [19] and were secondary to rhegmatogenous retinal detachment. The indications for vitrectomy in eyes with RD were giant breaks, macular breaks, and bullous retinal detachment with complex arrangement of breaks. The indications for vitrectomy in eyes with PDR were tractional retinal detachment, and/or nonclearing vitreous hemorrhage. In patients with PDR, the clinical ocular findings were graded at the time of vitrectomy for the presence or absence of patent new vessels on the retina or optic disc. Patients with active PDR were graded as such on the basis of visible, patent new vessels on the retina or optic disc or their absence (inactive PDR). Active PDR was present in 37 patients, and PDR was inactive in 51 cases (*table 1*). Vitreous humor samples were collected undiluted by manual suction into a syringe through the aspiration line of the vitrectomy, before opening the infusion line. The samples were centrifuged, and the supernatants were frozen at -40°C until assay. Epiretinal membranes were obtained from 18 patients with PDR and 5 patients with PVR during pars plana vitrectomy. Fourteen PDR membranes and 5 PVR membranes were fixed in 10% formalin solution and embedded in paraffin. Four PDR epiretinal membranes were immediately snap frozen in Tissue-Tek optimum cutting temperature (OCT) compound (Miles Laboratories, IN, USA) and maintained at -80°C until use. The study was conducted according to the tenets of the Declaration of Helsinki, and informed consent was obtained from all patients. The study was approved by the Research Center, College of Medicine, King Saud University.

Chemokine assays

Sandwich enzyme-linked immunosorbent assays (ELISAs) for chemokines were developed with the antisera included in *table 2*. The detection limits and reference chemokines used as a standard are also shown in *table 1*. A 96-well plate was coated overnight (4°C) with the primary antibody (Ab) in phosphate-buffered saline (PBS). Remaining protein binding sites on the plate were blocked for 1 hour (37°C) with blocking buffer (PBS containing 0.05% Tween 20 and 0.1% casein). Samples and standards were diluted in blocking buffer and transferred to the plate. After 1 hour of incubation (37°C), the secondary Ab was added as capturing Ab for another 1 hour. All intermediate washing steps were performed with PBS containing 0.05% Tween 20. Depending on whether the secondary Ab was produced in mouse, rabbit or was biotinylated, the detection was performed with a corresponding peroxidase-conjugated polyclonal Ab (Jackson Immuno Research Laboratories, West Grove, PA, USA) and 3,3',5,5'-tetramethylbenzidine dihydrochloride hydrate. Measurement of the optical density at 450 nm with a microplate photometer allowed the calculation of the chemokine concentration in the samples by the corresponding standard curve.

Immunohistochemical staining

After deparaffinization, endogenous peroxidase was abolished with 2% hydrogen peroxide in methanol for

Table 1
Characteristics of the patients with proliferative diabetic retinopathy (PDR)
(88 patients)

• Age (y)	Mean \pm SD, 49.3 \pm 12.1 (range, 24- 72)
• Sex	
- Male	64 (72.7%)
- Female	24 (27.3)
• Type of diabetes	
- IDDM	61 (69.3%)
- NIDDM	27 (30.7%)
• Duration of diabetes (y)	Mean \pm SD, 16.9 \pm 6.6 (range, 5-33)
• Glycosylated hemoglobin (%)	Mean \pm SD, 8.35 \pm 1.33 (range, 6.7-13.3)
• Activity of PDR	
- Active	37 (42%)
- Inactive	51 (58%)
• Indications for vitrectomy	
- Tractional retinal detachment	39 (44.3%)
- Combined vitreous hemorrhage and tractional retinal detachment	26 (29.5%)
- Vitreous hemorrhage	23 (26.2%)

IDDM = insulin-dependent diabetes mellitus; NIDDM = non-insulin-dependent diabetes mellitus.

20 minutes, and nonspecific background staining was blocked by incubating the sections for 5 minutes in normal swine serum. For MCP-1 detection, antigen retrieval was performed by boiling the sections in 10 mM Tris-EDTA buffer [pH 9] for 30 minutes. For CD34, α -SMA and SDF-1 detection, antigen retrieval was performed by boiling the sections in 10mM citrate buffer [pH 6] for 30 minutes. Subsequently, the sections were incubated with the monoclonal antibodies listed in *table 3*. Optimal working concentration and incubation time for the antibodies were determined earlier in pilot experiments. For CD34, MCP-1, and SDF-1 immunohis-

tochemistry, the sections were incubated for 30 minutes with goat anti-mouse immunoglobulins conjugated to peroxidase-labeled dextran polymer (EnVision⁺; Dako, Carpinteria, CA, USA). For α -SMA immunohistochemistry, the sections were incubated for 30 minutes with the biotinylated secondary antibody and reacted with the avidin-biotinylated peroxidase complex (Dako). The reaction product was visualized by incubation for 10 minutes in 0.05 M acetate buffer at pH 4.9, containing 0.05% 3-amino-9-ethylcarbazole (Sigma-Aldrich, Bornem, Belgium) and 0.01% hydrogen peroxide, resulting in

Table 2
Sandwich enzyme-linked immunosorbent assays against human chemokines

Chemokine	Application	Antibody type	Source ^a	Concentration	Detection limit	Standard protein
CCL1/I-309	Primary	Monoclonal mouse	R&D Systems	1 μ g/mL	0.05 ng/mL	Rec I-309
	Secondary	Biotinylated polyclonal goat	(Quantikine kit)	0.1 μ g/mL		(R&D Systems)
CCL2/MCP-1	Primary	Monoclonal mouse	R&D Systems	1.7 μ g/mL	0.4 ng/mL	Rec MCP-1
	Secondary	Biotinylated polyclonal goat	R&D Systems	0.05 μ g/mL		[20]
CCL3/MIP-1 α	Primary	Polyclonal goat	R&D Systems	2 μ g/mL	5 ng/mL	Rec MIP-1 α
	Secondary	Monoclonal mouse	Biosource	0.125 μ g/mL		(R&D Systems)
CCL4/MIP-1 β	Primary	Polyclonal rabbit	Peprtech	0.2 μ g/mL	2 ng/mL	Rec MIP-1 β
	Secondary	Monoclonal mouse	R&D Systems	0.17 μ g/mL		(R&D Systems)
CCL7/MCP-3	Primary	Polyclonal rabbit	Rega Institute	0.16 μ g/mL	0.5 ng/mL	Syn MCP-3
	Secondary	Monoclonal mouse	R&D Systems	0.5 μ g/mL		[21]
CCL8/MCP-2	Primary	Polyclonal rabbit	Rega Institute	6 μ g/mL	0.5 ng/mL	Rec MCP-2
	Secondary	Monoclonal mouse	R&D Systems	0.125 μ g/mL		[20, 22]
CXCL5/ENA-78	Primary	Polyclonal rabbit	Peprtech	1.6 μ g/mL	4 ng/mL	Rec ENA-78
	Secondary	Polyclonal goat	R&D Systems	3 μ g/mL		(Peprtech)
CXCL6/GCP-2	Primary	Polyclonal rabbit	Peprtech	1 μ g/mL	0.025	Syn GCP-2 [23]
	Secondary	Monoclonal mouse	R&D Systems	0.25 μ g/mL	ng/mL	
CXCL10/IP-10	Primary	Monoclonal mouse	R&D Systems	0.5 μ g/mL	0.1 ng/mL	Rec IP-10
	Secondary	Biotinylated polyclonal goat	R&D Systems	0.17 μ g/mL		(Peprtech)
CXCL11/I-TAC	Primary	Polyclonal rabbit	Peprtech	0.17 μ g/mL	0.25 ng/mL	Rec I-TAC
	Secondary	Monoclonal mouse	R&D Systems	0.5 μ g/mL		(R&D Systems)

syn = synthetic, rec = recombinant.

^a Location of manufacturers: Biosource Europe (Nivelles, Belgium); R&D Systems (Abingdon, UK); Peprtech (Rocky Hill, NJ, USA).

Table 3
Monoclonal antibodies used in this study

Primary antibody	Dilution	Incubation time	Source ^a
• Anti-CD34 (clone My10)	1/10	60 minutes	BD Biosciences
• Anti- α -smooth muscle Actin (clone 1A4)	1/100	30 minutes	Dako
• Anti- CCL2/MCP-1 (clone 23002)	1/25	120 minutes	R&D Systems
• Anti-CXCL12/ SDF-1 (clone 79018)	1/50	30 minutes	R&D Systems
• Anti-CXCR3 (clone 49801)	1/25	120 minutes	R&D Systems

^a Location of manufacturers: BD Biosciences (San Jose, CA, USA); Dako (Glostrup, Denmark); R&D Systems (Abingdon, UK).

bright-red immunoreactive sites. The slides were weakly counterstained with Harris hematoxylin. Finally, the sections were rinsed with distilled water and cover-slipped with glycerol.

For CXCR3 immunohistochemistry, 5 μ m cryostat sections were dried overnight at room temperature, fixed in absolute acetone for 10 minutes and then treated with 2% hydrogen peroxide in methanol for 3 minutes to block endogenous peroxidase activity. After rinsing three times in PBS at pH 7.2 for 15 minutes, the slides were incubated with the monoclonal antibody (*table 3*). After washing with PBS, the sections were incubated for 30 minutes with EnVision⁺, peroxidase, Mouse (Dako). The slides were washed again with PBS and the reaction product was visualized by incubation for 10 minutes in 0.05M acetate buffer at pH 4.9, containing 0.05% 3-amino-9-ethylcarbazole and 0.01% hydrogen peroxide, resulting in bright-red immunoreactive sites. The slides were weakly counterstained with Harris hematoxylin. Finally, the sections were rinsed with distilled water and coverslipped with glycerol. Omission or substitution of the primary antibody with an irrelevant antibody of the same species, and staining with chromogen alone were used as negative controls. Sections from patients with Crohn's disease were used as positive controls.

Quantitation

Blood vessels and cells were counted in five representative fields, using an eyepiece calibrated grid with 40x magnification. With this magnification and calibration, the blood vessels and cells present in an area of 0.33 x 0.22 mm were counted.

Statistical analysis

The data were analyzed using the Mann-Whitney test, the Chi-square test, correlation analysis, and one way analysis of variance (ANOVA). The Mann-Whitney test was used to compare means for two independent groups. The Chi-square test was used for comparing proportions when analyzing data for two categorical variables. One way analysis of variance was used to compare means for several groups. Data transformations were applied to the data to reduce variance before conducting the ANOVA. When there was no appropriate transformation, the one way ANOVA was conducted using the non-parametric Kruskal-Wallis test. Kruskal-Wallis test was conducted using the program 3S from the BMDP statistical software. For post-ANOVA, pairwise comparisons of means, based on the Kruskal-Wallis test, the critical value for the Z-statistics was $Z = 2.39$ at 5% level of significance and 3

groups of means to be compared. Therefore, test values exceeding 2.39 indicated statistical significance. Test for linear trend was used to confirm whether the incidence of IP-10 detection consistently increased with successively higher levels of MCP-1. The Pearson correlation coefficient was computed to investigate the linear relationship between the variables investigated. A p value less than 0.05 indicated statistical significance.

RESULTS

Chemokine levels in vitreous humor and paired serum samples

Among the chemokines analyzed, only MCP-1 and IP-10 were detected in vitreous humor samples. The results are summarized in *tables 4 and 5*. MCP-1 was detected in all vitreous humor samples (100%), and in 45 (25.4%) of 177 serum samples; the incidence rates of detection differed significantly ($P < 0.001$; Chi-square test). The incidence rates of detection of MCP-1 in vitreous humor samples from RD, PVR and PDR patients were significantly higher than in serum samples ($p < 0.001$ for all comparisons; Chi-square test). When all patients were considered, the mean MCP-1 level in vitreous humor samples was significantly higher than that in serum samples ($p < 0.001$; Mann-Whitney test). Mean MCP-1 levels in vitreous humor samples from RD, PVR, and PDR patients were significantly higher than in serum samples ($p < 0.001$ for all comparisons; Mann-Whitney test) (*table 4*). There was no correlation between vitreous humor and serum MCP-1 levels in the entire study group ($r = -0.0201$; $p = 0.7913$), in RD patients ($r = 0.1712$; $p = 0.2029$), in PVR patients ($r = -0.2074$; $p = 0.2630$), and in PDR patients ($r = -0.0108$; $p = 0.9211$).

Mean MCP-1 levels in vitreous humor samples differed significantly between RD, PVR, and PDR patients ($p = 0.0002$; Kruskal-Wallis test). Post-ANOVA mean comparisons indicated that mean MCP-1 levels in patients with PVR and PDR were significantly higher than the mean levels in patients with RD ($Z = 4.05$; 2.45, respectively). When patients with PDR were divided into those with active disease and those with inactive disease, the mean MCP-1 level in vitreous humor samples from active PDR cases was significantly higher than that in inactive PDR cases ($p = 0.0224$; Mann-Whitney test) (*table 5*).

IP-10 was detected in 95 (53.7%) of 177 vitreous humor samples from all patients, and in 29 (16.4%) of 177 serum samples, and the incidence rates of detection differed significantly ($p < 0.001$; Chi-square test). The incidence rates for IP-10 detection in vitreous humor samples *versus*

Table 4
Summary data for chemokine levels

	CCL2/MCP-1		CXCL10/IP-10	
	No. of samples with detectable levels (%)	Levels detected (ng/mL) (Mean ± SD)	No. of samples with detectable levels (%)	Levels detected (ng/mL) (Mean ± SD)
• All patients (n = 177)				
Vitreous	177 (100)	1.78 ± 1.64	95 (53.7)	0.45 ± 0.64
Serum	45 (25.4)	0.19 ± 0.07	29 (16.4)	0.14 ± 0.05
p value	< 0.001 ^a	< 0.001 ^a	< 0.001*	0.0035*
• RD patients (n = 57)				
Vitreous	57 (100)	1.16 ± 0.73	18 (31.6)	0.16 ± 0.17
Serum	10 (17.5)	0.18 ± 0.08	7 (12.3)	0.13 ± 0.04
p value	< 0.001*	< 0.001*	0.0236*	0.5752
• PVR patients (n = 32)				
Vitreous	32 (100)	2.74 ± 2.46	24 (75)	0.5 ± 0.55
Serum	7 (21.9)	0.22 ± 0.1	3 (9.4)	0.16, 0.07, 0.11
p value	< 0.001*	< 0.001 ^a	< 0.001*	NA
• PDR patients (n = 88)				
Vitreous	88 (100)	1.83 ± 1.54	53 (60.2)	0.53 ± 0.75
Serum	28 (31.8)	0.18 ± 0.06	19 (21.6)	0.14 ± 0.05
p value	< 0.001*	< 0.001*	< 0.001*	0.0102*

RD = rhegmatogenous retinal detachment with no PVR; PVR = retinal detachment complicated by proliferative vitreoretinopathy; PDR = proliferative diabetic retinopathy; NA = not applicable.

^a Statistically significant at 5% level of significance. Statistical evaluation is described in detail in the text of the result section.

serum samples differed significantly in RD, PVR, and PDR patients ($p = 0.0236$; < 0.001 ; < 0.001 , respectively; Chi-square test) (table 4). For the vitreous humor samples, the incidence rates of detection in RD, PVR, and PDR cases differed significantly ($p < 0.001$; Chi-square test). Further analysis indicated that the incidences of detection of IP-10 in vitreous humor samples from PVR and PDR patients were significantly higher than in RD cases ($p < 0.001$; 0.0017, respectively; Chi-square test). When patients with PDR were divided into those with active disease and those with inactive disease, the incidence of detection of IP-10 in vitreous humor samples from active PDR cases was significantly higher than that in inactive PDR cases ($p = 0.0214$; Chi-square test) (table 5).

When all patients were considered, the mean IP-10 level in vitreous humor samples was significantly higher than that found in serum samples ($p = 0.0035$; Mann-Whitney test). However, the mean IP-10 level in vitreous humor samples from RD patients did not differ significantly from that found in serum samples ($p = 0.5752$; Mann-Whitney test). The mean IP-10 level in vitreous humor samples from PVR patients was $0.5 = 0.55$ ng/mL, but IP-10 was de-

tected in only 3 out of 32 serum samples from PVR patients. The mean IP-10 level in vitreous humor samples from PDR patients was significantly higher than that found in serum samples ($p = 0.0102$; Mann-Whitney test) (table 4). There was no correlation between vitreous humor and serum IP-10 levels in the entire study group ($r = 0.0397$; $p = 0.6019$), in RD patients ($r = -0.1501$; $p = 0.2650$), in PVR patients ($r = -0.1188$; $p = 0.5243$), and in PDR patients ($r = 0.1627$; $p = 0.1321$).

Mean IP-10 levels in vitreous humor samples differed significantly between RD, PVR, and PDR patients ($p = 0.0083$; Kruskal-Wallis test). Post-ANOVA mean comparisons indicated that mean IP-10 levels in patients with PVR and PDR were significantly higher than the mean level in patients with RD ($Z = 2.89$; 2.72, respectively). When patients with PDR were divided into those with active disease and those with inactive disease, the mean IP-10 level in vitreous humor samples from active PDR cases was higher than that found in inactive cases but the difference between the two means was statistically insignificant ($p = 0.2232$; Mann-Whitney test) (table 5).

Table 5
Summary data for chemokine levels in vitreous humor samples

	CCL2/MCP-1		CXCL10/IP-10	
	No. of samples with detectable levels (%)	Levels detected (ng/mL) (mean ± SD)	No. of samples with detectable levels (%)	Levels detected (ng/mL) (mean ± SD)
RD (n = 57)	57 (100)	1.16 ± 0.73	18 (31.6)	0.16 ± 0.17
PVR (n = 32)	32 (100)	2.74 ± 2.46	24 (75)	0.5 ± 0.55
PDR (n = 88)	88 (100)	1.83 ± 1.54	53 (60.2)	0.53 ± 0.75
p value		0.0002 ^a	< 0.001 ^a	0.0083 ^a
Active PDR (n = 37)	37 (100)	2.31 ± 1.88	28 (75.7)	0.75 ± 0.97
Inactive PDR (n = 51)	51 (100)	1.47 ± 1.12	25 (49)	0.30 ± 0.26
p value		0.0224*	0.0214 ^a	0.2232

RD = rhegmatogenous retinal detachment with no PVR; PVR = retinal detachment complicated by proliferative vitreoretinopathy; PDR = proliferative diabetic retinopathy.

^a Statistically significant at 5% level of significance. Statistical evaluation is described in detail in the text of the result section.

Table 6
Relationships between the incidence rates of IP-10 detection and MCP-1 levels in vitreous humor samples

CCL2/MCP-1 (ng/mL)	Incidence of CXCL10/IP-10 detection			
	All patients	RD	PVR	PDR
< 1.0	14/59 (23.7%)	4/24 (16.7%)	2/5 (40%)	8/30 (26.7%)
1.0 – 2.0	37/70 (52.9%)	7/26 (26.9%)	9/12 (75%)	21/32 (65.6%)
> 2.0	44/48 (91.6%)	7/7 (100%)	13/15 (86.7%)	24/26 (92.3%)
p value (Chi-square test)	< 0.001 ^a	< 0.001 ^a	0.1133	< 0.001 ^a
p value (test for linear trend)	< 0.001 ^a	< 0.001 ^a	0.05279	< 0.001 ^a

RD = rhegmatogenous retinal detachment with no PVR; PVR = retinal detachment complicated by proliferative vitreoretinopathy; PDR = proliferative diabetic retinopathy.
^a Statistically significant at 5% level of significance.

There was a significant association between the incidence of IP-10 detection and increased levels of MCP-1 in vitreous humor samples from all patients, and in vitreous humor samples from RD and PDR patients ($p < 0.001$ for all comparisons; Chi-square test and test for linear trend). However, the association between the incidence of IP-10 detection and increased levels of MCP-1 was not significant in vitreous humor samples from PVR patients (table 6).

Immunohistochemical localization of chemokines in epiretinal membranes from patients with PDR and PVR

There was no staining in the negative control slides (figure 1A). All formalin-fixed PDR membranes showed blood vessels positive for CD34 (figure 1B), with a mean number of 25.3 ± 16.4 (range, 2-64). Myofibroblasts expressing α -smooth muscle actin (α -SMA) were detected

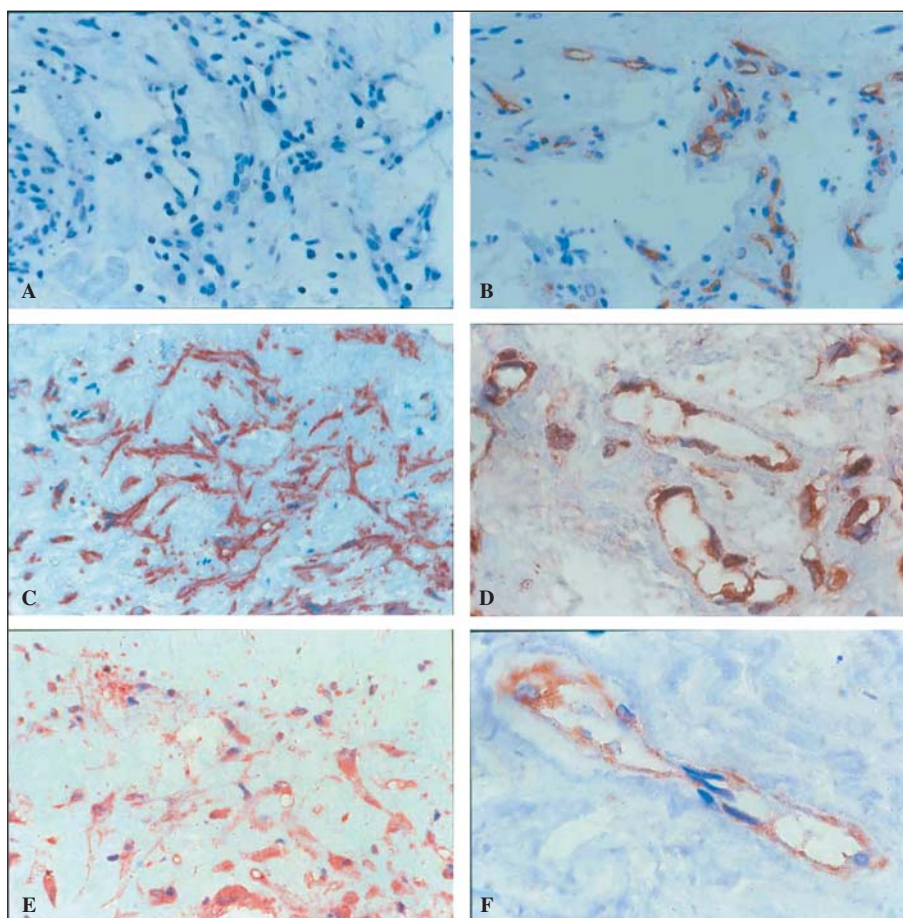


Figure 1

Proliferative diabetic retinopathy epiretinal membranes. **A)** Negative control slide that was treated identically with an irrelevant antibody showing no labelling (original magnification x 40). **B)** Immunohistochemical staining for CD34 showing blood vessels positive for CD34 (original magnification x 40). **C)** Immunohistochemical staining for α -smooth muscle actin showing strong immunoreactivity in myofibroblasts (original magnification x 40). **D)** Immuno-histochemical staining for monocyte chemoattractant protein-1 showing strong immunoreactivity on vascular endothelial cells (original magnification x 100). **E)** Immunohistochemical staining for monocyte chemoattractant protein-1 showing immunoreactivity in myofibroblasts (original magnification x 40). **F)** Immunohistochemical staining for stromal cell-derived factor-1 showing immunoreactivity on vascular endothelial cells (original magnification x 100).

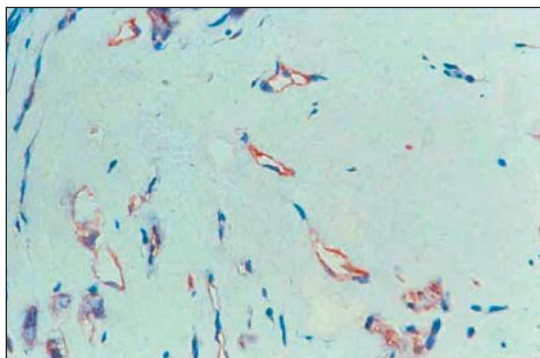


Figure 2

Proliferative diabetic retinopathy periretinal membrane. Immunohistochemical staining for CXCR3 showing immunoreactivity on vascular endothelial cells (original magnification x 40).

in all membranes (*figure 1C*), with a mean cell number of 49.1 ± 28.8 (range, 18-115). Strong MCP-1 immunoreactivity was noted on vascular endothelial cells in all specimens (*figure 1D*), with a mean cell number of 20.9 ± 11.4 (range, 2-37). MCP-1 immunoreactivity was also noted in large cells (*figure 1E*) in 12 (85.7%) membranes with a mean cell number of 27.5 ± 21.6 (range, 0-75). In serial sections, the distribution of cells expressing MCP-1 was similar to the distribution of myofibroblasts expressing α -SMA. There was a significant correlation between the number of blood vessels expressing CD34 and the number of blood vessels expressing MCP-1 ($r = 0.6049$; $p = 0.0285$), as well as the number of myofibroblasts expressing MCP-1 ($r = 0.7078$; $p = 0.0068$). In addition, there was a significant correlation between the number of myofibroblasts expressing α -SMA and the number of myofibroblasts expressing MCP-1 ($r = 0.8504$; $p = 0.0002$). Immunoreactivity for SDF-1 was present in 11 (78.6%) specimens, and was weaker than that for MCP-1. SDF-1 expression was noted on vascular endothelial cells (*figure 1F*) in 11 (78.6%) specimens, with a mean cell number of 6.9 ± 4.8 (range, 0-15). In serial sections, SDF-1 immunoreactivity was also noted in myofibroblasts expressing α -SMA in 5 (35.7%) specimens, with a mean cell number of 3.2 ± 5.0 (range, 0-17). The correlations between the number of blood vessels expressing CD34, the number of blood vessels expressing SDF-1 ($r = 0.4735$; $p = 0.0873$), and the number of myofibroblasts expressing

SDF-1 ($r = 0.1610$; $p = 0.5823$) were not significant. However, there was a significant correlation between the number of myofibroblasts expressing α -SMA and the number of myofibroblasts expressing SDF-1 ($r = 0.6159$; $p = 0.019$). Finally, immunoreactivity for CXCR3 was noted on vascular endothelial cells in all frozen PDR membranes (*figure 2*).

In PVR membranes, there was no immunoreactivity for CD34 in any of the specimens. Myofibroblasts expressing α -SMA were detected in all specimens (*figure 3A*), with a mean cell number of 79.0 ± 25.3 (range, 43-105). Strong MCP-1 immunoreactivity was noted in myofibroblasts expressing α -SMA in all membranes (*figure 3B*), with a mean cell number of 73.0 ± 30.0 (range, 46-120). Weaker immunoreactivity for SDF-1 was noted in myofibroblasts expressing α -SMA in 4 (80%) membranes, with a mean cell number of 13.4 ± 7.7 (range, 0-21). The numbers of cells expressing MCP-1, and SDF-1 were significantly higher in PVR membranes compared with PDR membranes ($p = 0.0125$; 0.0210 , respectively; Mann-Whitney test).

DISCUSSION

In the present study, the following three findings were demonstrated: 1) among the 6 CC chemokines and the 4 CXC chemokines studied, only the CC chemokine MCP-1, and the CXC chemokine IP-10 were detected in the vitreous humor samples from eyes with proliferative vitreoretinal disorders; 2) MCP-1, and IP-10 levels in the vitreous humor samples were significantly higher than serum levels, and there was no significant correlation between vitreous humor and serum levels, suggesting that MCP-1 and IP-10 in vitreous humor reflected local production; and 3) myofibroblasts in PDR and PVR membranes expressed MCP-1 and SDF-1, and vascular endothelial cells in PDR membranes expressed MCP-1 and SDF-1 and the chemokine receptor CXCR3.

Progressive fibrosis is a common pathological finding in various organs, resulting in organ failure. Recently, it was demonstrated that MCP-1, as well as its interaction with its major, mononuclear cell receptor CCR2, plays a pivotal role in mediating persistent mononuclear phagocyte infiltration that leads to chronic inflammatory/fibroproliferative diseases [24-26]. Blockade of MCP-

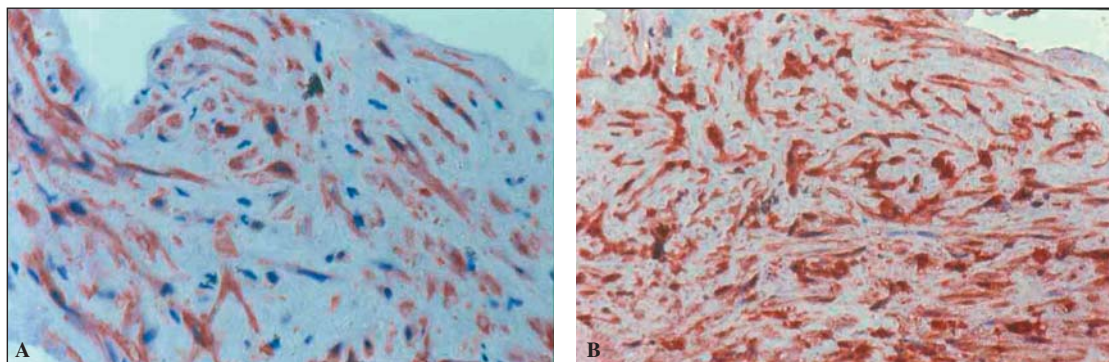


Figure 3

Proliferative vitreoretinopathy epiretinal membranes. **A**) Immunohistochemical staining for α -smooth muscle actin showing strong immunoreactivity in myofibroblasts. **B**) Immunohistochemical staining for monocyte chemoattractant protein-1 showing strong immunoreactivity in myofibroblasts (original magnification x 40).

1/CCR2 signaling reduced renal interstitial fibrosis in a rat model of renal fibrosis, with the concomitant decrease in the expression of MCP-1, transforming growth factor β , and type I collagen, and reduced CCR2-positive macrophages [26]. Furthermore, anti-MCP-1 gene therapy decreased bleomycin-induced pulmonary fibrosis in mice [25]. MCP-1 deficient mice displayed significantly delayed wound re-epithelialization, and wound angiogenesis, and reduced collagen synthesis [27] suggesting that MCP-1 plays a critical role in wound healing. Recent evidence suggests that MCP-1 might participate in the fibrotic process by inducing the secretion of extracellular matrix components. Gharaee-Kermani *et al.* [28] showed that MCP-1 promotes collagen expression by fibroblasts in a transforming growth factor β -dependent manner.

Recently, MCP-1 has been recognized as an angiogenic chemokine [29-31]. Salcedo *et al.* [30] showed that the angiogenic effect of MCP-1 does not require inflammatory leukocytes. *In vivo* angiogenesis assays showed that MCP-1-induced angiogenesis was as potent as that induced by vascular endothelial growth factor (VEGF) [29], which is implicated strongly in the development of retinal and iris neovascularization in PDR [9]. The angiogenic effect of MCP-1 was completely inhibited by a VEGF inhibitor, suggesting that MCP-1-induced angiogenesis is mediated through pathways involving VEGF [29]. In a mouse model of oxygen-induced ischemic retinopathy, MCP-1 levels increased after ischemia, and was localized in the hypoxic inner retina. Neutralizing antibodies against MCP-1 reduced retinal neovascularization [32]. Our results of increased levels of MCP-1 in the vitreous humor samples from patients with PVR or with PDR are consistent with previous reports [4-6]. Furthermore, we found that MCP-1 levels in vitreous humor samples from active PDR cases were significantly higher than those in inactive PDR cases. Collectively, these findings provide evidence that increased MCP-1 expression contributes to the development of neovascularization and fibrosis in proliferative vitreoretinal disorders.

Another aim of the present study was to determine which cell types express MCP-1, and SDF-1 in epiretinal membranes. Using immunohistochemistry, we demonstrated for the first time that MCP-1, and SDF-1 proteins were specifically localized in vascular endothelial cells and myofibroblasts. In addition, we demonstrated that the number of blood vessels expressing the panendothelial marker CD34 in PDR membranes correlated significantly with the number of blood vessels, and the number of myofibroblasts expressing MCP-1. These immunohistochemical results are consistent with the detection of significantly higher levels of MCP-1 in vitreous humor samples from patients with active PDR compared with vitreous humor samples from patients with inactive PDR. Our results are in agreement with a previous report that demonstrated increased expression of MCP-1 mRNA in endothelial cells obtained from the aorta of diabetic patients [33]. Diabetes results in various metabolic and biochemical abnormalities in the retina such as increased oxidative stress [34], and accumulation of advanced glycation end products [35], which have been shown to induce the expression of MCP-1 in vascular endothelial cells [36, 37]. In addition, high glucose enhanced the production of MCP-1, and induced reactive oxygen species in vascular endothelial cells [38]. Recently, Yamada *et al.* [39] dem-

onstrated that VEGF increased MCP-1 mRNA levels in cultured endothelial cells, and that MCP-1 participates in VEGF-induced angiogenesis and vascular leakage. On the other hand, Hong *et al.* [29] showed that MCP-1 induced VEGF expression in endothelial cells. These data suggest a positive regulatory feedback loop between VEGF and MCP-1 expression by vascular endothelial cells in mediating angiogenesis.

Several studies have demonstrated that SDF-1 induces an angiogenic effect *in vitro* and *in vivo*, and that VEGF and SDF-1 efficiently and synergistically induce *in vivo* angiogenesis and vascular endothelial cell migration [16-18]. New vessel formation induced *in vivo* by VEGF was markedly reduced by specific neutralizing antibodies directed at SDF-1 [17]. Recently, Brooks *et al.* [7] showed increased SDF-1 levels in vitreous humor from patients with PDR, supporting a role for SDF-1 in the pathogenesis of PDR. *In vitro* studies have demonstrated that VEGF and basic fibroblast growth factor enhance SDF-1 expression in vascular endothelial cells [17]. Furthermore, SDF-1 appears to be induced in endothelium undergoing vascular remodeling in the context of tumor angiogenesis and vessel recanalization [17]. Recently, circulating endothelial progenitor cells mobilized from the bone marrow were detected in the peripheral blood and recruited to foci of neovascularization where they form new blood vessels *in situ* through a process called vasculogenesis. The chemokine SDF-1 and its receptor CXCR4 were identified as critical mediators for the ischemia-specific recruitment of circulating endothelial progenitor cells. It was also shown that SDF-1 expression in ischemic tissue was primarily localized to endothelial cells, creating high local levels of SDF-1, and that its expression was directly regulated by hypoxia-inducible factor-1. SDF-1 expression facilitated adhesion of progenitor cells to ischemic endothelium and induced their migration [40]. Taken together, the expression of SDF-1 by vascular endothelial cells in PDR membranes indicates a potentially important role for SDF-1 in the pathogenesis of retinal neovascularization in diabetic patients.

The presence of α -SMA-expressing myofibroblasts in PVR and PDR epiretinal membranes has been previously reported [41]. In the present study, we demonstrated that MCP-1, and SDF-1 were expressed in myofibroblasts in PVR and PDR membranes and that the number of myofibroblasts expressing α -SMA significantly correlated with the numbers of MCP-1 and SDF-1 expressing myofibroblasts in PDR membranes. Similarly, in other diseases characterized by excessive fibrosis such as coal workers pneumoconiosis [42], and systemic sclerosis [43], MCP-1 was expressed by fibroblasts and myofibroblasts. Recently, Orimo *et al.* [44] demonstrated that carcinoma-associated myofibroblasts produce increased levels of SDF-1, which is responsible for recruiting endothelial progenitor cells into carcinoma, enhancing angiogenesis and thus promoting tumor growth. It was also demonstrated that hypoxia is a potent inducer of SDF-1 production by synovial fibroblasts [45], and that rheumatoid fibroblasts overexpress SDF-1, which supports CD4⁺ and CD8⁺ T cell migration within synovial tissue [46]. These data suggest a role for myofibroblast-secreted MCP-1 and SDF-1 in mediating angiogenesis and recruitment of leukocytes into preretinal membranes.

In the present study, IP-10 levels and the incidence of its detection in the vitreous humor samples from eyes with PVR and PDR were significantly greater than the levels of IP-10 and the incidence of its detection in RD cases. A previous report documented elevated IP-10 levels in vitreous humor samples from patients with PDR [8]. To our knowledge, however, this is the first report of IP-10 in PVR. Furthermore, we demonstrated that IP-10 levels and its incidence of detection were higher in vitreous humor samples from active PDR cases compared with vitreous humor samples from patients with inactive PDR. This result is in contrast to the previous report, in which Elner *et al.* [8] demonstrated higher IP-10 levels in inactive PDR cases. However, they studied only six cases with inactive PDR. Recently, Boulday *et al.* [47] demonstrated that VEGF, an established angiogenesis factor in PDR [9], induced IP-10 expression *in vitro* and *in vivo*. These findings indicate that VEGF-induced augmentation of IP-10 expression is a major mechanism underlying its proinflammatory function in immunity.

Increased expression of IP-10 has also been shown in other fibrotic disorders [48-50]. Suzuki *et al.* [49] examined the expression pattern of IP-10 in a rat model of renal tubulointerstitial fibrosis. They demonstrated that the expression of IP-10 mRNA showed an early increase, which coincided with the onset of infiltration of lymphocytes, followed by a gradual decrease to the control level. Marstik *et al.* [50] described a similar profile of increased IP-10 expression throughout the early phase of peritoneal wound healing followed by its decline at more advance stages of healing that coincided with an increased incidence of adhesion. These data are in general agreement with our results, which demonstrated higher levels and incidence of detection of IP-10 in active PDR cases compared with inactive cases. Several studies reported that IP-10 is a potent inhibitor of angiogenesis [51-53] and may have an inhibitory effect on fibrosis [48, 51]. IP-10 inhibits fibroblast chemotaxis and accumulation in fibrotic disorders, but has no direct effect on fibroblast proliferation [48, 51]. In addition, angiostatic, non-ELR CXC chemokines, including IP-10, can inhibit neovascularization induced by angiogenic chemokines [52, 54, 55]. In the present study, we demonstrated the expression of the chemokine receptor CXCR3, the cognate receptor for IP-10 [15], by vascular endothelial cells in PDR epiretinal membranes. There is increasing evidence that the expression of CXCR3 is enhanced during the proliferative stage of the angiogenesis process [12].

Taken together, our results suggest that elevated levels of IP-10 in vitreous humor from patients with PVR and PDR, as well as its interaction with its receptor CXCR3, potentially negatively regulates fibrosis/angiogenesis in proliferative vitreoretinal disorders. In addition, the significant association between the incidence of IP-10 detection and increased levels of MCP-1 suggest that the cross talk between MCP-1 and IP-10 appears to be critical and has a direct role in coordinating the events that lead to fibrosis/angiogenesis in proliferative vitreoretinal disorders. Further studies are necessary to provide better understanding of the relationship between chemokines and their receptors, which might contribute to the identification of molecular targets for preventing undesirable angiogenesis/fibrosis in the eye.

Acknowledgements. The authors thank Mr. Johan Van Even for technical assistance, and Ms. Connie B. Unisa-Marfil for secretarial work.. This work was supported by the College of Medicine, Research Center, King Saud University, Fund for Scientific Research of Flanders (F.W.O.-Vlaanderen), the Concerted Research Actions (G.O.A.) of the Regional Government of Flanders, the InterUniversity Attraction Poles Programme-Belgian Science Policy (I.U.A.P.), and the European Union 6FP, EC contract INNOCHEM. Sofie Struyf is a senior research assistant of the F.W.O.-Vlaanderen.

REFERENCES

- Esser P, Heimann K, Wiedemann P. Macrophages in proliferative vitreoretinopathy and proliferative diabetic retinopathy: differentiation of subpopulations. *Br J Ophthalmol* 1993; 77: 731-3.
- Tang S, Le-Ruppert KC. Activated T lymphocytes in epiretinal membranes from eyes of patients with proliferative diabetic retinopathy. *Graefes Arch Clin Exp Ophthalmol* 1995; 233: 21-5.
- Charteris DG, Hiscott P, Grierson I, Lightman SL. Proliferative vitreoretinopathy: lymphocytes in periretinal membranes. *Ophthalmology* 1992; 99: 1364-7.
- Capeans C, De Rojas MV, Lojo S, Salorio MS. C-C chemokines in the vitreous of patients with proliferative vitreoretinopathy and proliferative diabetic retinopathy. *Retina* 1998; 18: 546-50.
- Elner SG, Elner VM, Jaffe GJ, Stuart A, Kunkel SL, Strieter RM. Cytokines in proliferative diabetic retinopathy and proliferative vitreoretinopathy. *Curr Eye Res* 1995; 14: 1045-53.
- Abu El-Asrar AM, Van Damme J, Put W, Veckeneer M, Dralands L, Billiau A, Missotten L. Monocyte chemoattractant protein-1 in proliferative vitreoretinal disorders. *Am J Ophthalmol* 1997; 123: 599-606.
- Brooks Jr. HL, Caballero Jr. S, Newell CK, Steinmetz RL, Watson D, Segal MS, Harrison JK, Scott EW, Grant MB. Vitreous levels of vascular endothelial growth factor and stromal-derived factor 1 in patients with diabetic retinopathy and cystoid macular edema before and after intraocular injection of triamcinolone. *Arch Ophthalmol* 2004; 122: 1801-7.
- Elner SG, Strieter R, Bian ZM, Kunkel S, Mokhtarzaden L, Johnson M, Lukacs N, Elner VM. Interferon-induced protein 10 and interleukin 8: C-X-C chemokines present in proliferative diabetic retinopathy. *Arch Ophthalmol* 1998; 116: 1597-601.
- Miller JW, Adamis AP, Aiello LP. Vascular endothelial growth factor in ocular neovascularization and proliferative retinopathy. *Diabetes Metab Rev* 1997; 13: 37-50.
- Watanabe D, Suzuma K, Kurimoto M, Kiryu J, Kita M, Suzuma I, Ohashi H, Ojima T, Murkami T, Kobayashi T, Masua S, Nagao M, Yoshimura N, Tkagi H. Erythropoietin as a retinal angiogenic factor in proliferative diabetic retinopathy. *N Engl J Med* 2005; 353: 782-92.
- Struyf S, Proost P, Van Damme J. Regulation of the immune response by the interaction of chemokines and proteases. *Adv Immunol* 2003; 81: 1-44.
- Salcedo R, Oppenheim JJ. Role of chemokines in angiogenesis: CXCL12/SDF-1 and CXCR4 interaction, a key regulator of endothelial cell responses. *Microcirculation* 2003; 10: 359-70.
- Agostini C, Gurrieri C. Chemokine/cytokine cocktail in idiopathic pulmonary fibrosis. *Proc Am Thorac Soc* 2006; 3: 357-63.
- Ong VH, Evans La, Shiwen X, Fisher IB, Rajkumar V, Abraham DJ, Black CM, Denton CP. Monocyte chemoattractant protein 3 as a mediator of fibrosis: Overexpression in systemic sclerosis and the type 1 tight-skin mouse. *Arthritis Rheum* 2003; 48: 1979-91.
- Murphy PM, Baggiolini M, Charo IF, Hebert CA, Horuk R, Matsushima K, Miller LH, Oppenheim JJ, Power CA. International Union of Pharmacology. XXII. Nomenclature for chemokine receptors. *Pharmacol Rev* 2000; 52: 145-76.

16. Mirshahi F, Pourtau J, Li H, Muraine M, Trochon V, Legrand E, Vannier J-P, Soria J, Vasse N, Soria C. SDF-1 activity on microvascular endothelial cells: consequences on angiogenesis in in vitro and in vivo models. *Thromb Res* 2000; 99: 587-94.
17. Salvucci O, Yao L, Villalba S, Sajewicz A, Pittaluga S, Tosato G. Regulation of endothelial cell branching morphogenesis by endogenous chemokine stromal-derived factor-1. *Blood* 2002; 99: 2703-11.
18. Kryczek I, Lange A, Mottram P, Alvarez X, Cheng P, Hogan M, Moons L, Wei S, Zou L, Machelon V, Emilie D, Terrassa M, Lackner A, Curiel TJ, Carmeliet P, Zou W. CXCL12 and vascular endothelial growth factor synergistically induce neoangiogenesis in human ovarian cancers. *Cancer Res* 2005; 65: 465-72.
19. Retina Society Terminology Committee. The classification of retinal detachment with proliferative vitreoretinopathy. *Ophthalmology* 1983; 90: 121-5.
20. Struyf S, Van Collie E, Paemen L, Paemen L, Put W, Lenaerts JP, Proost P, Opdenakker G, Van Damme J. Synergistic induction of MCP-1 and -2 by IL-1 beta and interferons in fibroblasts and epithelial cells. *J Leukoc Biol* 1998; 63: 364-72.
21. Proost P, Van Leuven P, Wuyts A, Ebberink R, Opdenakker G, Van Damme J. Chemical synthesis, purification and folding of the human monocyte chemoattractant proteins MCP-2 and MCP-3 into biologically active chemokines. *Cytokine* 1995; 7: 97-104.
22. Van Coillie E, Proost P, Van Aelst L, Struyf S, Polfliet M, De Meester I, Harvey DJ, Van Damme J, Opdenakker G. Functional comparison of two human monocyte chemoattractant protein-2 isoforms, role of the amino-terminal pyroglutamic acid and processing by CD26/dipeptidyl peptidase IV. *Biochemistry* 1998; 37: 12672-80.
23. Wuyts A, Van Osselaer N, Haelens A, Samson I, Herdewijn P, Ben-Baruch A, Oppenheim JJ, Proost P, Van Damme J. Characterization of synthetic human granulocyte chemoattractant protein 2: usage of chemokine receptors CXCR1 and CXCR2 and in vivo inflammatory properties. *Biochemistry* 1997; 36: 2716-23.
24. Belperio JA, Keane MP, Burdick MD, Lynch III JP, Xue YY, Berlin A, Ross DJ, Kunkel SL, Charo IF, Strieter RM. Critical role for the chemokine MCP-1/CCR2 in the pathogenesis of bronchiolitis syndrome. *J Clin Invest* 2001; 108: 547-56.
25. Inoshima I, Kuwano K, Hamada N, Hagimoto N, Yoshimi M, Maeyama T, Takeshita A, Kitamoto S, Egashira K, Hara N. Anti-monocyte chemoattractant protein-1 gene therapy attenuates pulmonary fibrosis in mice. *Am J Physiol Lung Cell Mol Physiol* 2004; 286: L1038-L1044.
26. Wada T, Furuichi K, Sakai N, Iwata Y, Kitagawa K, Ishida Y, Kondo T, Hashimoto H, Ishiwata Y, Mukaida N, Tomosugi N, Matsushima K, Egashira K, Yokoyama H. Gene therapy via blockade of monocyte chemoattractant protein-1 for renal fibrosis. *J Am Soc Nephrol* 2004; 15: 940-8.
27. Low QE, Drugea IA, Duffner LA, Quinn DG, Cook DN, Rollins BJ, Kovacs EJ, DiPietro LA. Wound healing in MIP-1 alpha (-/-) and MCP-1 (-/-) mice. *Am J Pathol* 2001; 159: 457-63.
28. Gharaee-Kermani M, Denholm EM, Phan SH. Costimulation of fibroblast collagen and transforming growth factor beta 1 gene expression by monocyte chemoattractant protein-1 via specific receptors. *J Biol Chem* 1996; 271: 17779-84.
29. Hong KH, Ryu J, Han KH. Monocyte chemoattractant protein-1-induced angiogenesis is mediated by vascular endothelial growth factor-A. *Blood* 2005; 105: 1405-7.
30. Salcedo R, Ponce ML, Young HA, Wasserman YK, Ward JM, Kleinman HK, Oppenheim JJ, Murphy WJ. Human endothelial cells express CCR2 and respond to MCP-1: direct role of MCP-1 in angiogenesis and tumor progression. *Blood* 2000; 96: 34-40.
31. Kim MY, Byeon CW, Hong KH, Han KH, Jeong S. Inhibition of angiogenesis by the MCP-1 (monocyte chemoattractant protein-1) binding peptide. *FEBS Lett* 2005; 579: 1597-601.
32. Yosida S, Yosida A, Ishibashi T, Elnor SG, Elnor VM. Role of MCP-1 and MIP-1 alpha in retinal neovascularization during post ischemic inflammation in a mouse model of retinal neovascularization. *J Leukoc Biol* 2003; 73: 137-44.
33. Feng L, Matsumoto C, Schwartz A, Schmidt AM, Stern DM, Pile-Spellman J. Chronic vascular inflammation in patients with type 2 diabetes. *Diabetes Care* 2005; 28: 379-84.
34. Kowluru RA. Retinal metabolic abnormalities in diabetic mouse: comparison with diabetic rat. *Curr Eye Res* 2002; 24: 123-8.
35. Stitt AW. The role of advanced glycation in the pathogenesis of diabetic retinopathy. *Exp Mol Pathol* 2003; 75: 95-108.
36. Lakshminarayanan V, Lewallen M, Frangogiannis NG, Evans AI, Wedin KE, Michael LH, Entman ML. Reactive oxygen intermediates induce monocyte chemoattractant protein-1 in vascular endothelium after brief ischemia. *Am J Pathol* 2001; 159: 1301-11.
37. Inagaki Y, Yamagishi S, Okamoto T, Takeuchi M, Amano S. Pigment epithelium-derived factor prevents advanced glycation end products-induced monocyte chemoattractant protein-1 production in microvascular endothelial cells by suppressing intracellular reactive oxygen species generation. *Diabetologia* 2003; 46: 284-7.
38. Takaishi H, Taniguchi T, Takahashi A, Ishikawa Y, Yokoyama M. High glucose accelerates MCP-1 production via p38 MAPK in vascular endothelial cells. *Biochem Biophys Res Commun* 2003; 305: 122-8.
39. Yamada M, Kim S, Egashira K, Takeya M, Ikeda T, Mimura O, Iwao H. Molecular mechanism and role of endothelial monocyte chemoattractant protein-1 induction by vascular endothelial growth factor. *Arterioscler Thromb Vasc Biol* 2003; 23: 1996-2001.
40. Ceradini DJ, Gurtner GC. Homing to hypoxia: HIF-1 as a mediator of progenitor cell recruitment to injured tissue. *Trends Cardiovasc Med* 2005; 15: 57-63.
41. Bochaton-Piallat M-L, Kapetanios AD, Donati G, Redard M, Gabbiani G, Pournaras CJ. TGF-beta 1, TGF-beta receptor II and ED-A fibronectin expression in myofibroblast of vitreoretinopathy. *Invest Ophthalmol Vis Sci* 2000; 41: 2336-42.
42. Boitelle A, Gosset P, Capin MC, Vanhee D, Marquette CH, Wallaert B, Gosselin B, Tonnel AB. MCP-1 secretion in lung from nonsmoking patients with coal worker's pneumoconiosis. *Eur Respir J* 1997; 10: 557-62.
43. Yamamoto T, Eckes B, Hartmann K, Krieg T. Expression of monocyte chemoattractant protein-1 in the lesional skin of systemic sclerosis. *J Dermatol Sci* 2001; 26: 133-9.
44. Orimo A, Gupta PB, Sgroi DC, Arenzana-Seisdedos F, Delaunay T, Naeem R, Carey VJ, Richardson AL, Weinberg RA. Stromal fibroblasts present in invasive human breast carcinomas promote tumor growth and angiogenesis through elevated SDF-1/CXCL12 secretion. *Cell* 2005; 121: 335-48.
45. Hitchon C, Wong K, Ma G, Reed J, Lyttle D, El-Gabalawy H. Hypoxia-induced production of stromal cell-derived factor 1 (CXCL12) and vascular endothelial growth factor by synovial fibroblasts. *Arthritis Rheum* 2002; 46: 2587-97.
46. Bradfield PF, Amft N, Vernon-Wilson E, Exley AE, Parsonage G, Rainger GE, Nash GB, Thomas AMC, Simmons DL, Salmon M, Buckley CD. Rheumatoid fibroblast-like synoviocytes overexpress the chemokine stromal cell-derived factor 1 (CXCL12) which supports distinct patterns and rates of CD4+ and CD8+ T cell migration within synovial tissue. *Arthritis Rheum* 2003; 48: 2472-82.
47. Boulday G, Haskova Z, Reinders ME, Pal S, Briscoe DM. Vascular endothelial growth factor induced signaling pathways in endothelial cells that mediate overexpression of the chemokines IFN-gamma-inducible protein of 10KDa in vitro and in vivo. *J Immunol* 2006; 176: 3098-107.

48. Tayer AM, Kradin RL, LaCamera P, Bercury SD, Campanella GS, Leary CP, Polosukhin V, Zhao LH, Sakamoto H, Blackwell TS, Luster AD. Inhibition of pulmonary fibrosis by the chemokine IP-10/CXCL10. *Am J Respir Cell Mol Biol* 2004; 31: 395-404.
49. Suzuki K, Kanabayashi T, Nakayama H, Doi K. Kinetics of chemokines and their receptors in mercuric chloride-induced tubulointerstitial lesions in Brown Norway rats. *Exp Mol Pathol* 2003; 75: 58-67.
50. Marstik M, Kotseos K, Chunfeng MA, Chegini N. Increased expression of interferon-inducible protein-10 during surgically induced peritoneal injury. *Wound Rep Reg* 2003; 11: 120-6.
51. Keane MP, Belperio JA, Arenberg DA, Burdick MD, Zu ZJ, Xue YY, Strieter RM. IFN- γ -inducible protein-10 attenuates bleomycin-induced pulmonary fibrosis via inhibition of angiogenesis. *J Immunol* 1999; 163: 5686-92.
52. Strieter RM, Polverini PJ, Kunkel SL, Arenberg DA, Burdick MD, Kasper J, Dzuiba J, Van Damme J, Walz A, Marriott D, Chan S-Y, Rocznik S, Shanafelt AB. The functional role of the ELR motif in CXC chemokine-mediated angiogenesis. *J Biol Chem* 1995; 270: 27348-57.
53. Angiolillo AL, Sgadari C, Taub DD, Liao F, Farber JM, Maheshwari S, Kleinman HK, Reaman GH, Tosato G. Human interferon-inducible protein 10 is a potent inhibitor of angiogenesis in vivo. *J Exp Med* 1995; 182: 155-62.
54. Struyf S, Burdick MD, Proost P, Van Damme J, Strieter RM. Platelets release CXCL4L1, a nonallelic variant of the chemokine platelet factor-4/CXCL4 and potent inhibitor of angiogenesis. *Circ Res* 2004; 95: 855-7.
55. Proost P, Schutyser E, Menten P, Struyf S, Wuyts A, Opdenakker G, Dethoux M, Parmentier M, Durinx C, Lambeir AM, Neyts J, Liekens S, Maudgal PC, Billiau A, Van Damme J. Amino-terminal truncation of CXCR3 agonists impairs receptor signaling and lymphocyte chemotaxis, while preserving antiangiogenic properties. *Blood* 2001; 98: 3554-61.